Electronic supplementary information

(ESI)

New cyanido-bridged iron(II) spin crossover coordination polymers with unusual ladder-like topology: an alternative to Hofmann clathrates

Diana Visinescu,[1] Sergiu Shova,[2] Sergii I.Shylin,[3] Ghenadie Novitchi,[4] Delia-Laura Popescu[5] and Maria-Gabriela Alexandru[6,*]*

[1]*"Ilie Murgulescu" Institute of Physical Chemistry, Romanian Academy, Splaiul Independentei 202, Bucharest 060021, Romania.*
[2]*Petru Poni Institute of Macromolecular Chemistry, Romanian Academy, Aleea Grigore Ghica Vodă 41-A, RO-700487 Iasi, Romania*
[3]*Department of Chemistry – Ångström Laboratory, Uppsala University, 75120 Uppsala, Sweden*
[4]*Laboratoire National des Champs Magnétiques Intenses (LNCMI), Univ. Grenoble Alpes, EMFL, CNRS 38042 Grenoble, France. E-mail: ghenadie.novitchi@lncmi.cnrs.fr*
[5]*Inorganic Chemistry Laboratory, Faculty of Chemistry, University of Bucharest, Dumbrava Rosie 23, 020464, Bucharest, Romania*
[6]*Department of Inorganic Chemistry, Physical Chemistry and Electrochemistry, Faculty of Chemical Engineering and Biotechnologies, National University of Science and Technology Politehnica of Bucharest, 1-7 Gh. Polizu Street, 011061 Bucharest, Romania. E-mail: maria.alexandru@up.ro*
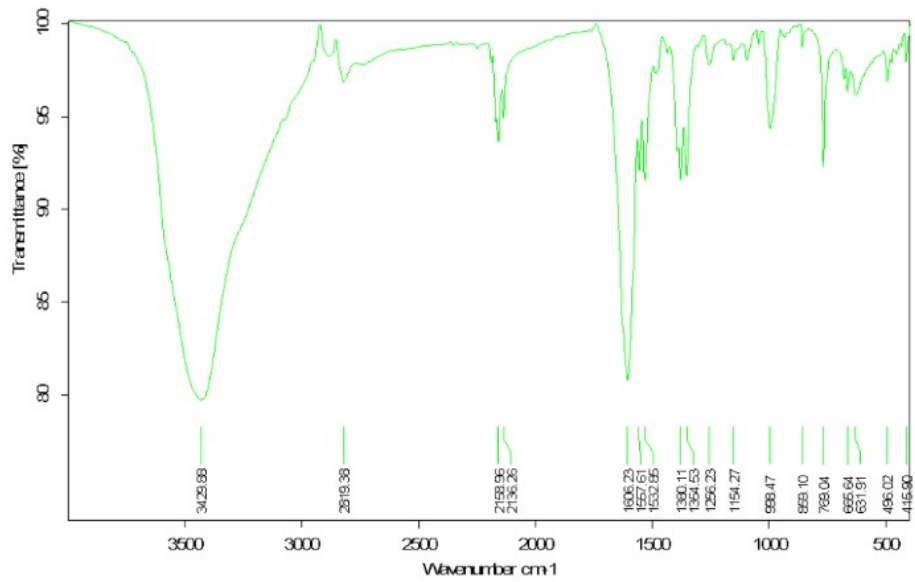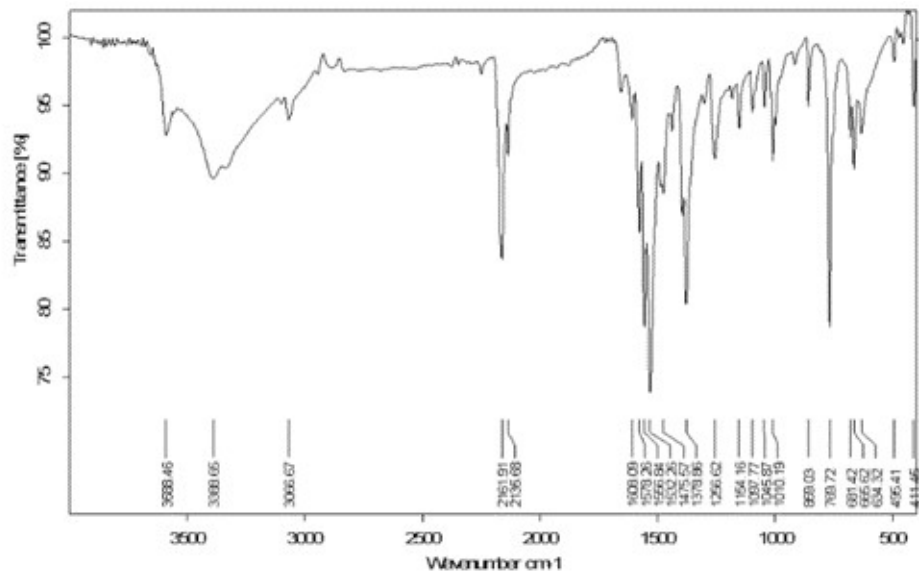
Fig. S1. FTIR spectrum of **1**
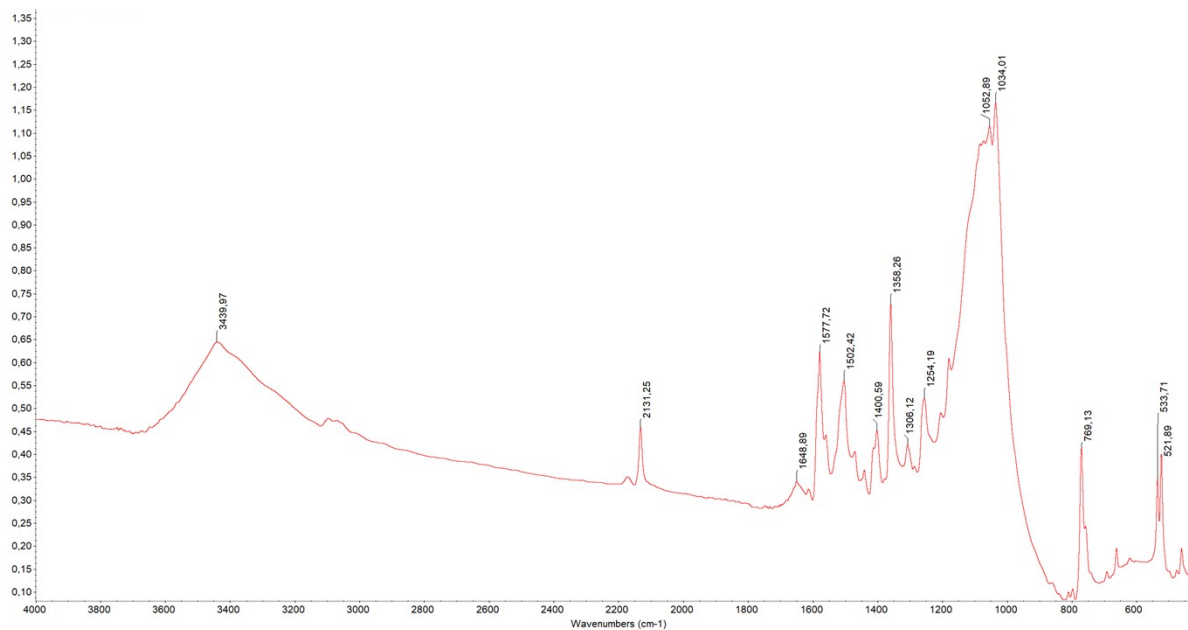

Fig. S2. FTIR spectrum of **2**

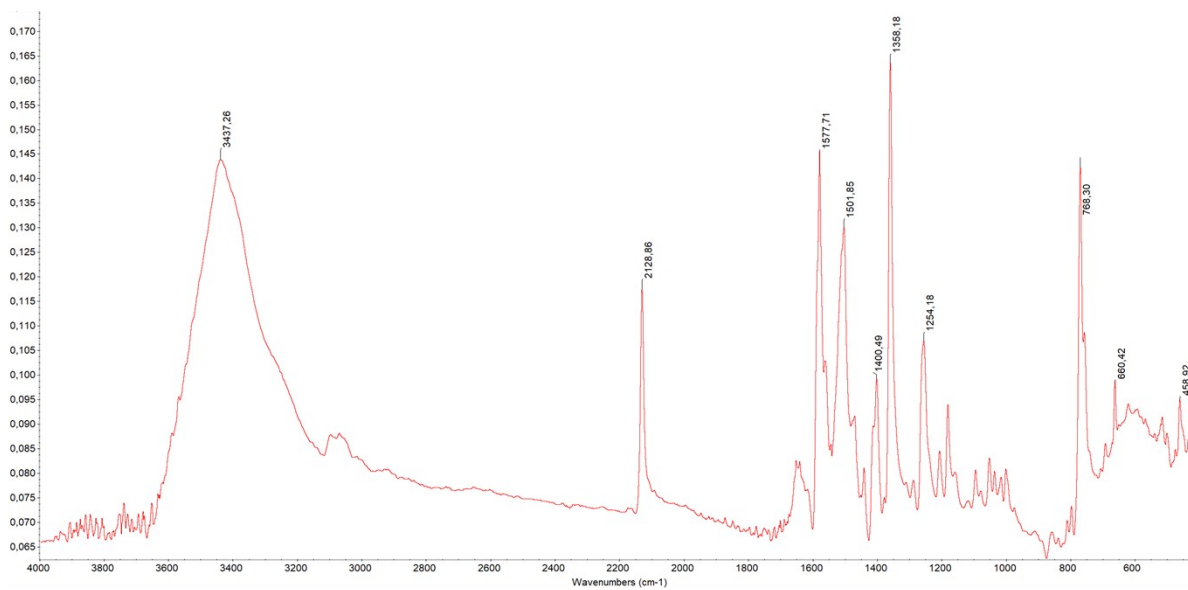**Fig. S3.** FTIR spectrum of **3**

Fig. S4. FTIR spectrum of **4**
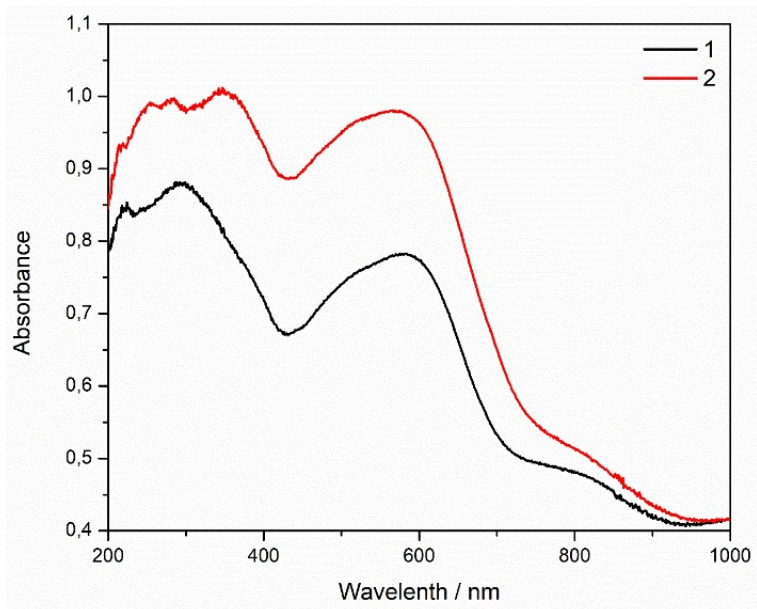
Fig. S5. Overlayed UV-Vis spectra of **1** and **2**
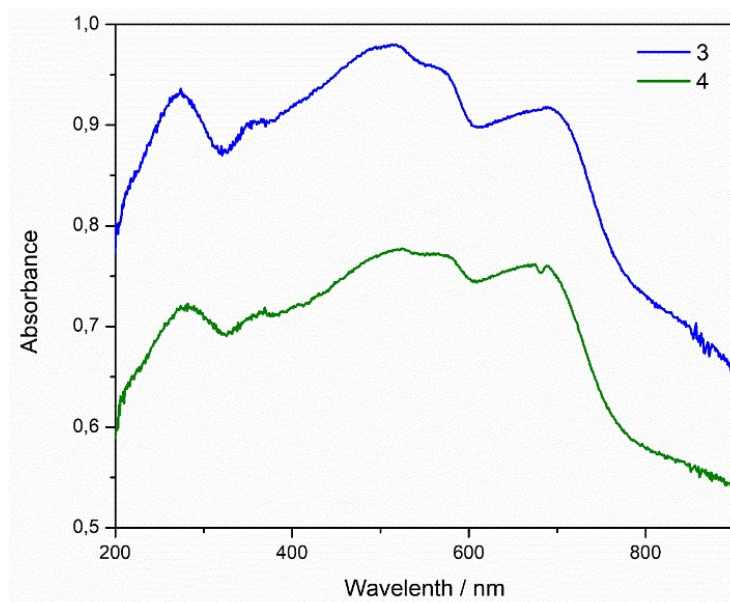

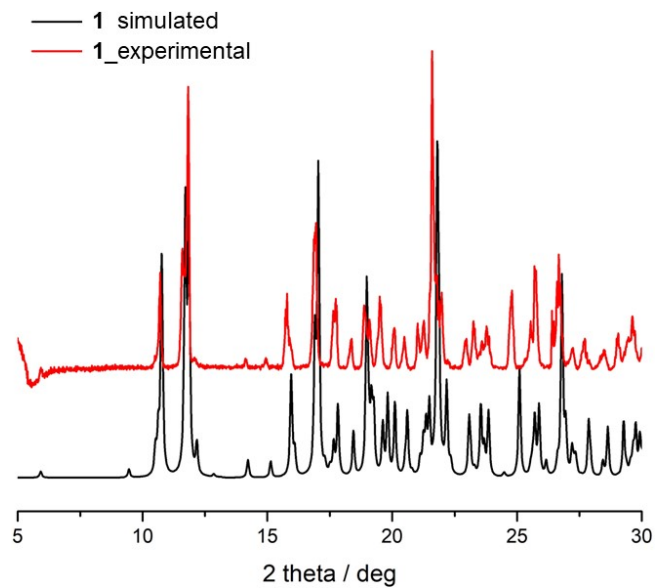**Fig. S6**. Overlayed UV-Vis spectra of **3** and **4**

Fig. S7. Experimental and calculated powder X-ray diffractograms at room temperature for **1.**
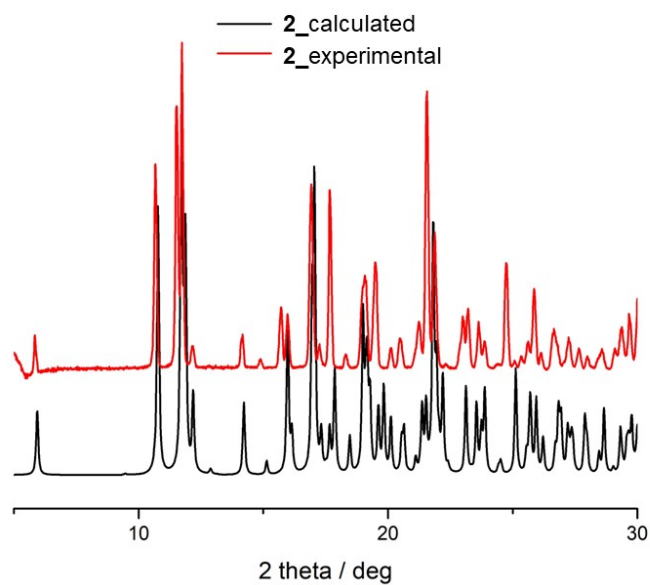

Fig. S8. Experimental and calculated powder X-ray diffractograms at room temperature for **2.**
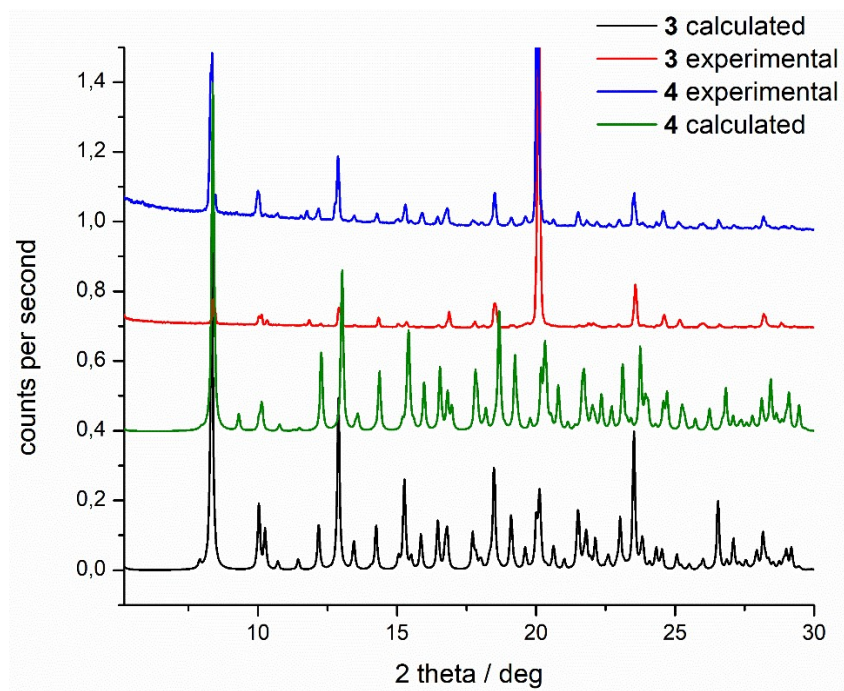
Fig. S9. Experimental and calculated powder X-ray diffractograms at room temperature for **3** and **4**.

Table S1. Bond lengths (Å) and angles (°) of the iron(II) and M(II) coordination environments in compounds **1** and **2**, respectively; M = Pd (**1**) and Pt (**2**).

	1 (180 K)	**1** (100 K)	**2** (120 K)
M1-C19	1.994(3)	1.992(5)	1.989(2)
M1-C20	1.995(3)	1.988(6)	1.994(2)
M1-C21	1.990(3)	2.002(5)	1.987(2)
M1-C22	1.990(3)	1.983(5)	1.984(2)
Fe1-N1	2.249(3)	2.166(4)	2.249(2)
Fe1-N2	2.129(3)	2.181(5)	2.2438(19)
Fe1-N3	2.246(3)	2.043(4)	2.2438(19)
Fe1-N7	2.090(3)	2.048(5)	2.101(2)
Fe1-N8 ^{a*}	2.111(3)	2.101(5)	
Fe1-N9 ^{a**}			2.091(2)
Fe1-N9 ^{b*}	2.180(3)	2.048(5)	
Fe1-N10 ^{b**}			2.1772(19)
C19-N7-Fe1	175.9(3)	174.5(5)	174.10(18)
C20-N8-Fe1 *,**	173.7(2)	173.5(4)	
C22-N10-Fe1 ^{c**}			172.74(18)
C21-N9-Fe1 ^{b*,**}	173.4(2)	175.2(4)	175.6(2)
N7-C19-M1	176.8(3)	177.7(5)	177.3(2)
N8-C20-M1	177.6(3)	176.9(5)	177.1(2)
N9-C21-M1	178.0(3)	178.1(4)	176.9(2)
N10-C22-M1	176.9(3)	176.4(4)	178.1(2)
N9 ^{b}-Fe1-N8 ^{a*,**}	174.55(10)	175.2(4)	
N1-Fe1-N2	72.62(9)	149.41(18)	145.65(7)
N3-Fe1-N1	145.60(9)	74.95(16)	72.63(7)
N3-Fe1-N2	72.99(9)	74.45(16)	73.03(7)
N7-Fe1-N9 ^{b*,**}	86.97(9)	88.13(17)	89.38(8)
N7-Fe1-N10 ^{a**}			174.24(7)
N8 ^{a}-Fe1-N2	100.79(9)	89.85(16)	
N10 ^{a}-Fe1-N2			86.54(7)
N9 ^{b}-Fe1-N1 *	89.65(9)	93.99(16)	
N10 ^{a}-Fe1-N1 **			89.81(7)
C19-M1-C21	90.72(11)	90.6(2)	90.19(9)
C20-M1-C19	90.41(11)	90.8(2)	90.88(9)
C22-M1-C21	87.91(11)	91.2(2)	90.73(9)
C20-M1-C22	90.91(11)	87.4(2)	88.17(9)

*(a) = 1-x, 1-y, 1-z; (b) = 2-x, -y, 1-z; **(a)= 1+x, y,-1+z; (b) = 1-x,1-y,1-z; (c) = -1+x,1+y,1+z

Table S2. Bond lengths (Å) and angles (°) of the iron(II) and M(II) coordination environments in compounds **3** and **4**, respectively; M = Pd (**3**) and Pt (**4**).

	3	4
Fe1-N1	2.009(5)	1.996(4)
Fe1-N2	1.864(5)	1.869(4)
Fe1-N3	2.001(5)	1.983(4)
Fe1-N7	1.992(5)	1.999(4)
Fe1-N8	1.862(5)	1.862(4)
Fe1-N9	2.014(5)	1.999(4)
M1-C37	-	2.006(5)
M1-C38	2.009(10)	2.000(8)
M1-C39	2.013(9)	1.994(5)
M2-C40	2.026(8)	2.004(5)
M2-C41	2.016(10)	-
N1-Fe1-N2	80.0(2)	79.56(15)
N1-Fe1-N3	158.9(2)	158.87(15)
N1-Fe1-N7	93.1(2)	92.26(15)
N1-Fe-N8	96.3(2)	98.90(15)
N1-Fe1-N9	92.4(2)	94.46(15)
N2-Fe1-N3	79.1(2)	79.61(15)
N2-Fe1-N7	101.6(2)	95.46(15)
N2-Fe-N8	176.1(2)	175.19(15)
N2-Fe1-N9	98.9(2)	105.31(15)
N3-Fe1-N7	88.3(2)	93.21(14)
N3-Fe1-N8	104.6(2)	102.14(15)
N3-Fe1-N9	93.6(2)	87.63(15)
N7-Fe1-N8	79.9(2)	80.01(15)
N7-Fe1-N9	159.4(2)	159.00(15)
N8-Fe1-N9	79.8(2)	79.31(15)
M1-C37-N13	-	177.0(4)
M1-C38-N14	-	176.1(9)
M1-C38-N13	177.1(9)	-
M1-C39-N14	178.3(8)	-
C37-M1-C37a**	-	180.0(2)
C37-M1-C38a	-	88.1(3)
C38-M1-C38a*	180.0(4)	180.0
C37-M1-C38	-	91.9(3)
C38-M1-C39	89.2(3)	-
C39-M2-C39b**	-	180.0
C39-M2-C40	-	91.41(19)
C39b-M2-C40**	-	88.59(19)
C39b-M2-C40b	-	91.41(19)
C39-M2-C40b**	-	88.59(19)
M2-C39-N15	-	178.8(5)
M2-C40-N16	-	179.2(4)
M2-C40-N15	176.2(7)	-
M2-C41-N16	178(3)	-
M2-C41a-N16a*	172(5)	-
C40-M2-C41	87.8(10)	-
C40-M2-C41b*	92.2(10)	-
C40b-M2-C40*,**	180.0	180.0

*(a) = 2-x, 1-y, 1-z; (b) = 2-x, 2-y, 2-z; **(a) = 2-x,1-y,1-z; (b) = -x, -y, -z

Table S3. Summary of the *SHAPE* analysis for the six-coordinated [$Fe^{II}N_6$] fragments in **1-4**

CN = 6[a]	**1** (180 K)	**1** (100 K)	**2**	**3**	**4**
HP-6	33.461	33.243	33.365	33.225	32.904
PPY-6	22.369	23.118	22.244	22.321	21.912
OC-6	**2.636**	**2.177**	**2.658**	**2.423**	**2.484**
TPR-6	11.367	11.768	11.206	11.129	10.886
JPPY-6	26.578	27.331	26.455	26.467	25.992

[a] PPY-6, C_{5v} Pentagonal pyramid; OC-6, O_h Octahedron; TPR-6, D_{3h} Trigonal prism; JPPY-5, C_{5v} Johnson pentagonal pyramid (J2)

Table S4. Selected intermolecular contacts for **1.**

D-H···A	d(D-H)/Å	d(H-A)/Å	d(D-A)/Å	D-H-A/°
O1W-H1WA···N6[x]	0.87	2.03	2.856(4)	159
O1W-H1WB···O2W	0.87	1.93	2.779(4)	164
O2W-H2WA···O1W[z]	0.87	1.89	2.748(4)	171
O2W-H2WB···N10[b]	0.87	2.31	3.140(4)	160

(x) = 1-*x*, 2-*y*, 2-*z*;(z) = -*x*, 2-*y*, 2-*z*;(b) = -*x*, 2-*y*, 1-*z*

Table S5. Selected intermolecular contacts for **2.**

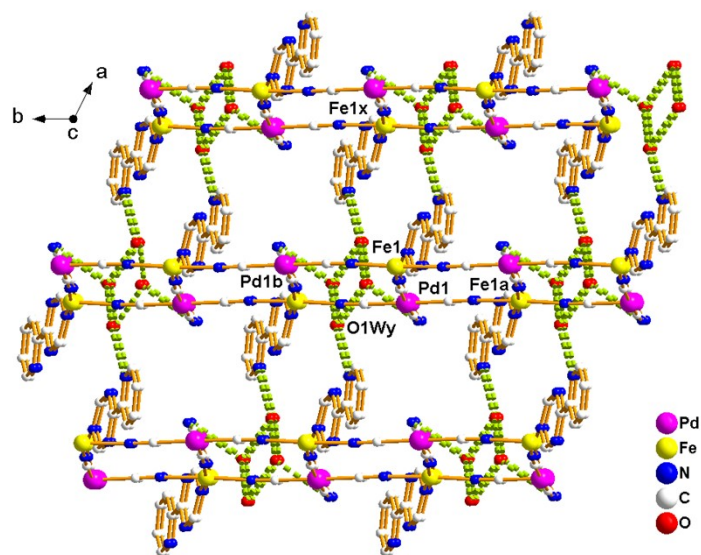| D-H···A	d(D-H)/Å	d(H-A)/Å	d(D-A)/Å	D-H-A/°
O2W-H1WA···N6	0.87	2.04	2.859(3)	157
O1W-H1WB···O2W	0.87	1.93	2.782(3)	165
O2W-H2WA···O1W[1]	0.87	1.89	2.750(3)	172
O2W-H2WB···N8[2]	0.87	2.30	3.126(3)	158

(1) =-*x*, -1-*y*, -*z*;(2) = -1-*x*, -1-*y*, 1-*z*

Fig. S10. Packing diagram of **1** showing the 3-D supramolecular network through H-bonds [symmetry coded: (b) = -x, 2-y, 1-z; (v) = x, y, 1+z; (w) = -1+x, y, z; (x) = 1-x, 2-y, 2-z; (y) = -x, 2-y, 2-z].
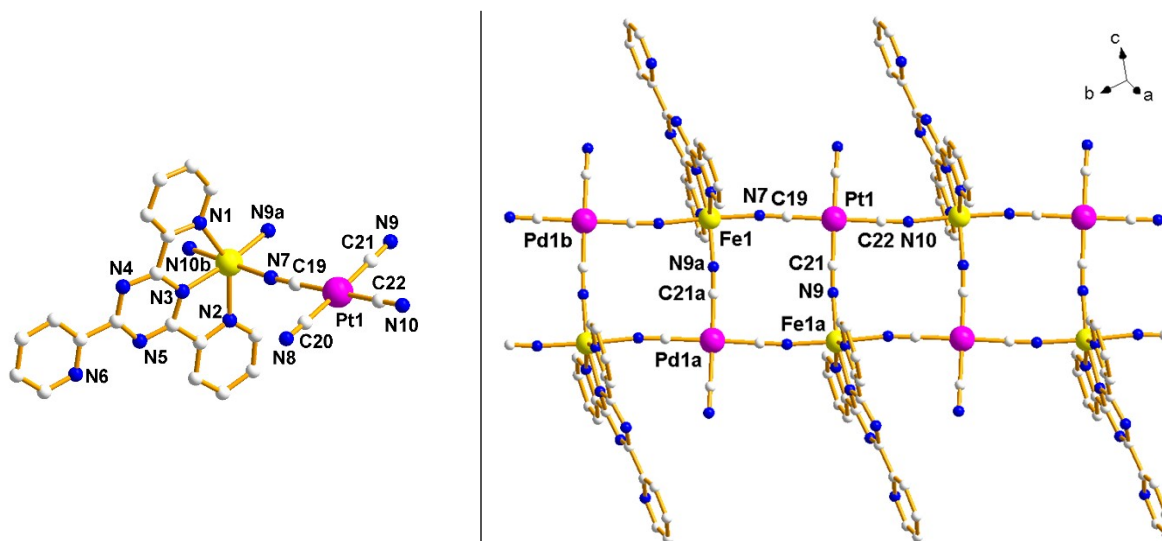

Fig.S11. Left. Asymmetric unit of **2**. Right. Fragment of the double chain **2**. (a) = 1-x, 1-y, -z; (b) = -1+x, 1+y, z.
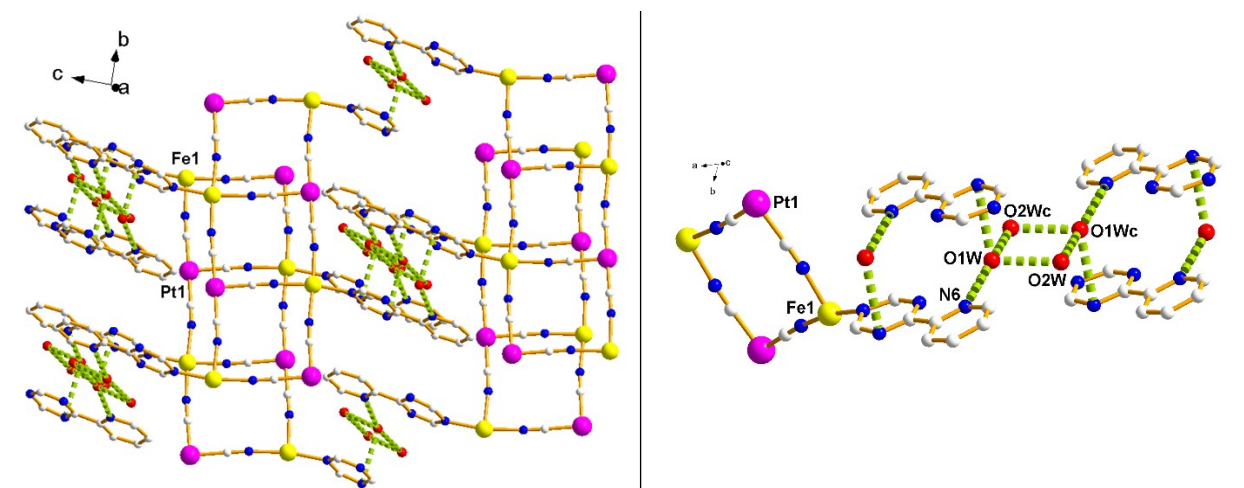
Fig. S12. Left: H-Bonds established in **2**. Right: Detail of crystal packing from the 3-D supramolecular network based on hydrogen bonding pattern in **2**. Symmetry code: (c) = -1-*x*, 1-*y*, 1-*z*.
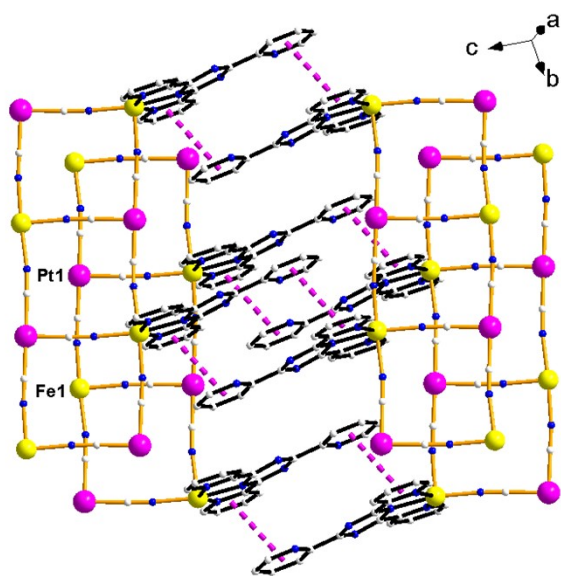

Fig. S13. π-π stacking interactions in **2** (the centroid-centroid distance of ca. 3.64 Å).

Table S6. Selected intermolecular contacts for **3**

D-H···A	d(D-H)/Å	d(H-A)/Å	d(D-A)/Å	D-H-A/°
O2W-H2WA···N6[h]	0.85	2.57	2.947(9)	108
O2W-H2WA···O4W[g]	0.85	2.57	2.935(19)	107
O2W-H2WB···N15	0.85	2.11	2.901(9)	154
O3W-H3WA···O3W[d]	0.85	2.45	2.890(19)	113
O3W-H3WA···O4W[d]	0.85	2.26	2.78(2)	120
O3W-H3WB···N16	0.85	2.52	2.797(19)	100
O1W-H1WA···O2W	0.85	2.12	2.944(9)	162
O1W-H1W···BN13[h]	0.85	2.13	2.933(11)	157

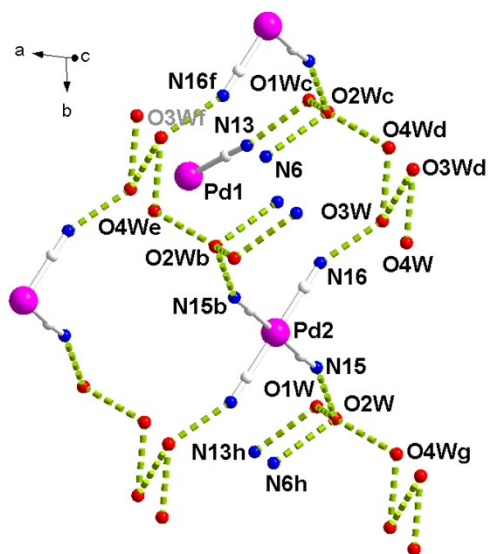(d) = 1-*x*, 1-*y*, 2-*z*; (g) = 1-*x*, 2-*y*, 2-*z*; (h) = *x*, 1+*y*, *z*.

Fig. S14. Detail of crystal packing from the 3-D supramolecular network based on hydrogen bonding pattern in **3**. Symmetry codes: (b) = 2-*x*, 1-*y*, 1-*z*; (c) = *x*, -1+*y*, *z*; (d) = 1-*x*, 1-*y*, 2-*z*; (e) = 1+*x*, *y*, *z*; (f) = 2-*x*, 1-*y*, 2-*z*; (g) = 1-*x*, 2-*y*, 2-*z*; (h) = *x*, 1+*y*, *z*.

Table S7. Selected intermolecular contacts for **4**

D-H···A	d(D-H)/Å	d(H-A)/Å	d(D-A)/Å	D-H-A/°
O2W-H2WA···O1W[1]	0.87	1.96	2.778(12)	156
O5W-H5WA···N15[3]	0.87	2.11	2.940(6)	159
O5W-H5WB···O4W	0.85	2.06	2.901(5)	170
O1W-H1WA···O2W[1]	0.85	2.44	2.778(12)	105
O1W-H1WB···N14	0.88	2.23	2.859(12)	128
O4W-H4WA···N12[4]	0.87	2.12	2.919(6)	152
O4W-H4WB···N13[5]	0.87	2.04	2.889(6)	164

(1) = 1-*x*, -*y*, 1-*z*; (2) = 1-*x*, 1-*y*, 1-*z*; (3) = 1-*x*, 1-*y*, -*z*; (4) = *x*, 1+*y*, *z*; (5) = 2-*x*, 1-*y*, 1-*z*.
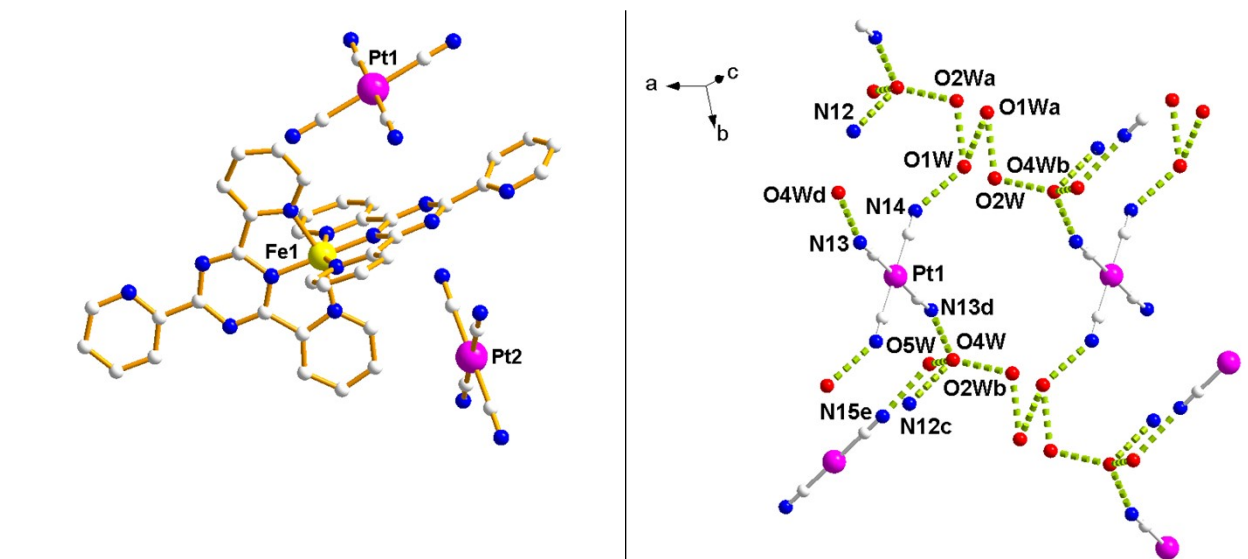

Fig. S15. Left: structure of **4**; Right: excerpt from the 3-D supramolecular network based on hydrogen bonding pattern in **4**. Symmetry codes: (a) = 1-*x*, -*y*, 1-*z*; (b) = 1-*x*, 1-*y*, 1-*z*; (c) = *x*, 1+*y*, *z*; (d) = 2-*x*, 1-*y*, 1-*z*; (e) = 1-*x*, 1-*y*, -*z*.
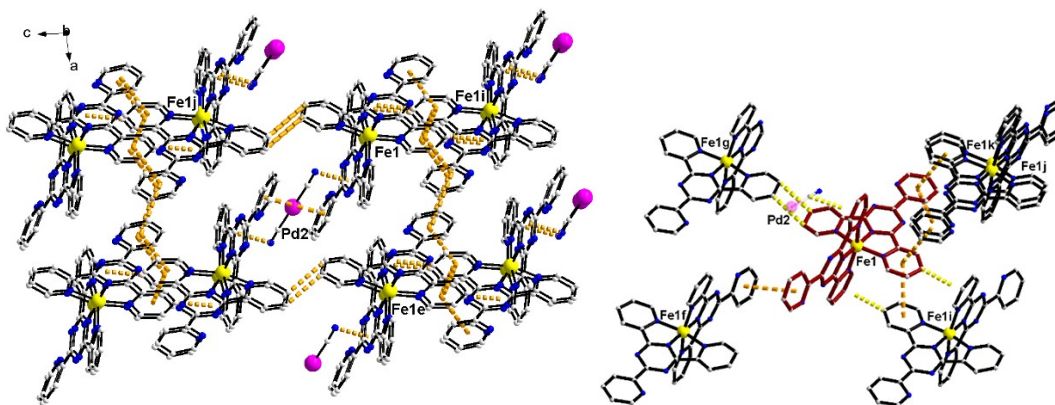
Fig. S16. Details of the crystal packing in **3** showing the offset and edge to face π-π stacking interactions established between peripheral pyridine and triazine rings of neighboring tptz ligands. Symmetry codes: (i) = 1-*x*, 1-*y*, 1-*z*; (j) = 1-*x*, 2-*y*, 1-*z*; (k) = -*x*, 2-*y*, 1-*z*.
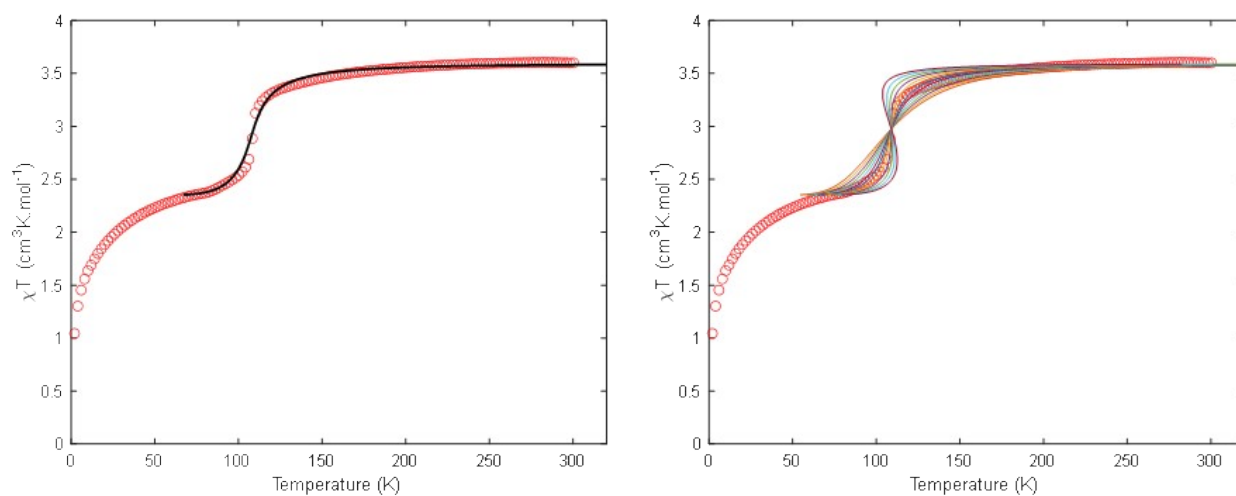

Fig. S17. Temperature dependence of magnetic susceptibility χT as a function of temperature (T) for compound **1**. The solid line represents the theoretical simulated value according to the Slichter-Drickamer model[52, 67] for the upper portion of the data of magnetic susceptibility with parameter indicated below: left, ΔH = 5.3 kJ/mol, ΔS = 48.62 J/mol γ = 1.2 kJ/mol, χT(HS) = 3.6 cm^3·mol^{-1}·K, χT(LS) = 2.35 cm^3·mol^{-1}·K; right, ΔH = 5.3 kJ/mol, ΔS = 48.62 J/mol, γ = 0, 0.2, 2.4 kJ/mol, χT(HS) = 3.6 cm^3·mol^{-1}·K, χT(LS) = 2.35 cm^3·mol^{-1}.